Title

STUDY OF THE (3He,t) REACTION MECHANISM VIA THE 38Ar (3He,t)38K REACTION AT 40 MeV

Author

Bruge, G.

Publication Date

1978-04-01

Submitted to Nuclear Physics

LBL-5823
Preprint

STUDY OF THE (^{3}He,t) REACTION MECHANISM VIA THE ^{38}Ar(^{3}He,t)^{38}K REACTION AT 40 MeV

G. Bruge, M. S. Zisman, A. D. Bacher,
R. Schaeffer, C. J. Zeippen, and J. M. Loiseaux

April 1978

Prepared for the U. S. Department of Energy
under Contract W-7405-ENG-48

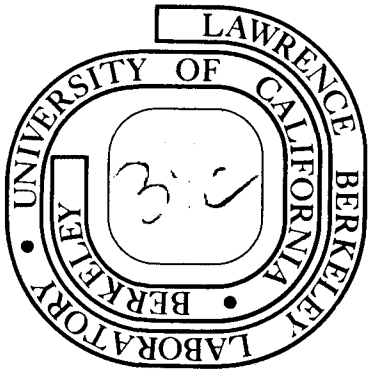

DISCLAIMER

STUDY OF THE (^{3}He,t) REACTION MECHANISM VIA THE ^{38}Ar(^{3}He,t)^{38}K REACTION AT 40 MeV*

G. Bruge,+ M. S. Zisman, A. D. Bacher,++ and R. Schaeffer+

Lawrence Berkeley Laboratory
University of California
Berkeley, California 94720

and

C. J. Zeippen+++ and J. M. Loiseaux

I.S.N. Grenoble
Grenoble, FRANCE

ABSTRACT

The ^{38}Ar(^{3}He,t)^{38}K reaction has been studied using a 40 MeV ^{3}He beam from the Berkeley 88-Inch cyclotron. Angular distributions for 26 levels are presented and theoretical analysis of the results has been carried out. Firstly, the conclusions of a macroscopic study of the ^{38}K level spectrum are presented. Secondly, the difficulties encountered using a one-step microscopic model to describe the five lowest states of ^{38}K are discussed. Thirdly, the improvements obtained by including two-step contributions in our microscopic model are shown and the importance of the transitions occurring via the [(^{3}He,α) + (α,t)] channel is emphasized.

1. Introduction

The present work is concerned with the "charge-exchange" reaction $^{38}Ar(^{3}He,t)^{38}K$ at 40 MeV. In recent years, increasing use has been made of the $(^{3}He,t)$ reaction as a spectroscopic tool.[1] In fact, it is a very powerful method of reaching nuclei which could otherwise be obtained only through transfer reactions. The charge-exchange reaction is generally described in terms of a microscopic model. In this framework, the $(^{3}He,t)$ reaction is very similar to a reaction involving inelastic scattering of a light projectile. However, in the case of $(^{3}He,t)$ charge exchange, the cross sections are very small, and multi-step processes can be a very important part of the reaction mechanism.[2,3]

Great progress has been made in our knowledge concerning the $(^{3}He,t)$ reaction mechanism. Usually, an effective force interacting between the projectile center-of-mass and the excited nucleon in the target is used.[4] It seems that enough information has been gathered in the case of nuclei with simple structures to enable one to make a reasonable choice of the force parameters and to start a spectroscopic study of more complex nuclei.[1,4-10]

It has been established that a tensor component is required in the nucleon-nucleon force if one wants to explain the angular distributions of unnatural parity levels.[6,7] In fact it seems that there are two distinct types of $(^{3}He,t)$ transitions which should show different sensitivity to the tensor term.[7] We have a great amount of information concerning the first type of transition and a very small amount concerning the second type. One of the reasons for studying the $^{38}Ar(^{3}He,t)^{38}K$ reaction is a desire to clarify our ideas about the apparent difference

between the two types of transitions. To this end we have compared the parameter values for the effective nucleon-nucleon force in an $(f_{7/2} \rightarrow f_{7/2})$ transition (type 1) for the reaction $^{48}Ca(^{3}He,t)^{48}Sc$ to those in a $(d_{3/2} \rightarrow d_{3/2})$ transition (type 2) for the reaction $^{38}Ar(^{3}He,t)^{38}K$, using various final states. Then, we increased the complexity of the wave functions representing the ^{38}Ar and ^{38}K nuclei, and also that of the transition operator by including two-step processes. We have concentrated our efforts on the first five levels of ^{38}K, since they are well separated in our experiment and their spins and parities are quite well known.

The first part of our theoretical analysis deals with the choice of optical parameters and with the assignment of transferred L-values to the ^{38}K levels populated through the $(^{3}He,t)$ reaction. Where possible comparison is made with other results.[11,12] Besides the usual one-step microscopic description of the $(^{3}He,t)$ reaction mechanism, it has also been possible to evaluate the importance of two-step transitions because of the existence of new codes allowing for coupled-channel calculations [in particular Ref. 13].

2. Experimental Procedure

The experiment was performed using a 40 MeV ^{3}He beam from the Berkeley 88-Inch cyclotron. The target was argon gas (enriched to 94.4% ^{38}Ar) at a pressure of 120 Torr which was contained in a cell having a thin (0.68 mg/cm^2) nickel entrance foil and a 2.1 mg/cm^2 Havar exit foil. Tritons were detected by telescopes consisting of 0.25 mm ΔE and 3 mm E detectors which fed a Goulding-Landis particle identifier.[14] The experimental spectrum is displayed in Fig. 1; the overall energy resolution is 75 keV FWHM. Triton groups corresponding to 26 states in ^{38}K up to an excitation energy of about 8 MeV have been observed; angular distributions have been measured from $\theta_{c.m.} = 11°$ to 50°.

3. Macroscopic Analysis of the Results

The unstable ^{38}K nucleus has been investigated through both decay experiments and direct pick-up reactions. Most of the results have been reviewed by Endt and Van der Leun.[11] Apart from a few low-lying states, the ^{38}K level structure appears to be rather complicated. The spins and parities of the first five states [i.e., ground state (3^+), 0.13 MeV (0^+,T=1), 0.46 MeV (1^+), 1.70 MeV (1^+), and 2.41 MeV (2^+, T=1)] are quite well established, but since those of the higher-lying states are rather ambiguous, one has to take the features of every experiment into account in order to derive proper information about them.

Taking advantage of the fact that they are well-understood, we shall use extensively the lowest five levels as reference states in the next sections to discuss the various possible mechanisms for the $^{38}Ar(^3He,t)^{38}K$ reaction. For the sake of simplicity, we shall consider first the macroscopic model in order to discuss the relationship between the assigned L-values and the spins and parities of the first five states of ^{38}K. The analysis will then be extended to the higher-lying states.

3.1 THE FIRST FIVE LEVELS OF ^{38}K AND THE CHOICE OF THE OPTICAL PARAMETERS.

We have tested extensively the influence of optical parameters on the angular distributions. Although any reasonable parameter choices give typical diffractive shapes which allow one to determine unambiguously the dominant L-transfer, the quality of the obtained fit obviously depends, to a certain extent, on the particular set chosen. The following procedure has thus been adopted:

a) Many optical potentials were tested and the angular distribution for the 0^+ IAS (isobaric analog state of the ^{38}Ar ground state), at 0.13 MeV in ^{38}K, was used as a probe of their adequacy.

b) For the other states, the transferred L-values were extracted from experiment. As we had a double aim, i.e., to get a good basis for the attribution of L-values to the higher-lying states, but also to test more elaborate reaction mechanisms for the lowest states, special care was taken to dispose of most of the ambiguities which could be due to the optical parameters.

In the case of the lowest five states, whose total angular momenta J are known, the usual selection rules for one-step processes were tested:

$$(-)^{\Delta L} = \pi \begin{cases} \Delta L = J \text{ for natural-parity states.} \\ \Delta L = J+1 \text{ for unnatural-parity states.} \end{cases}$$

All the calculations were performed using the macroscopic formalism included in the code DWUCK.[15] The same optical parameters were taken for both the incoming channel and the form factor. Qualitatively, four sets of parameters, taken, respectively, from Refs. 5,16,17 and 18, give a good fit for the 0^+ state [see Fig. 2]. The angular distributions for the other states (1^+ to 3^+) are displayed in Fig. 3, which shows the fits obtained with the first and the last potential sets only. The calculated cross sections have been arbitrarily normalized to the maximum of the experimental angular distribution.

One can see that:

a) Satisfactory agreement is obtained for the 3^+ ground state with an L=4 angular distribution. The second maximum is essentially in phase with an L=2 curve, but no L=4 + L=2 mixture gave a good overall fit; the amount of L=2 which is necessary to fit the second maximum completely spoils the agreement at forward angles.

b) No agreement can be obtained for the 0.458 MeV 1_1^+ state if we restrict ourselves to the L=0 or L=2 patterns allowed in a one-step transition. On the contrary, a reasonable fit is given only by an L=1 calculated curve, in contradiction with the parity selection rule. One must note that this case is different from the previous one in that no agreement at all can be obtained even for a portion of the experimental angular distribution with the expected L=2 or L=0 curves. We were unable to find an optical potential set which could solve this problem without spoiling the agreement for the other states (in particular for the other 1^+ state). This is reminiscent of the L=1 shape found for some $0^+ \rightarrow 0^+$ transitions observed in the (^{3}He,t) reaction,[19] and may be considered as a signature of the presence of second-order effects, in particular the [(^{3}He,α) + (α,t)] process.[2,3,20]

c) In contrast with the previous case, good agreement is obtained for the 1_2^+ state at 1.704 MeV with a calculated L=2 angular distribution, as is usual for such a (^{3}He,t) transition.[5] Summing L=2 and L=0 calculated curves does not particularly improve the fit because only a very weak L=0 contribution is allowed by the experimental data. One should notice that the measured angular distribution for this state is out of phase with the data for the 0.458 MeV 1_1^+ state [see Fig. 3].

d) Only the slope is properly reproduced for the 2^+ level at 2.405 MeV which does not have a diffractional structure, although the calculated angular distribution predicts one. This lack of structure for the 2^+ state is not explained in this model. The nature of the optical potentials we chose can be questioned but good fits have been obtained using them for other nuclei (^{48}Sc and ^{52}Mn). We believe that

this particular shape of the 2^+ angular distribution can be attributed to the presence of second-order contributions, although we would not consider this to be as clear evidence for their existence as is the change in shape of the 0.458 MeV 1^+_1 angular distribution.

As we have not found a potential set which could give very good agreement for all five experimental distributions, we adopt the set of parameters which provides the best overall agreement. One can see, looking at Figs. 2 and 3, that the differences between the displayed fits are unimportant, except perhaps in the case of the 2^+ level, for which the slope is slightly better if one uses potential set d) instead of set a). Nevertheless, it is fair to say that a great number of optical parameter sets are essentially equivalent as far as our macroscopic analysis is concerned. Potentials including spin-orbit terms have been used and the non-locality corrections available in the code DWUCK[15] have been tested. They do not markedly affect the final results. Thus, we shall concentrate below on the two parameter sets given in Table I.

3.2 HIGHER-LYING LEVELS OF ^{38}K.

The experimental angular distributions for the higher-lying states of ^{38}K are displayed in Figs. 4a and 4b. One can see that most of them show significant diffraction shapes. The curves are theoretical angular distributions computed with the code DWUCK and arbitrarily normalized to the experimental data. The figure gives results obtained with the second set of optical parameters of Table I. The quality of fits and the conclusions one can draw would not be altered if one used the first set of Table I. Eight angular distributions, however, do not display typical

patterns. Thus no L-value has been attributed to these states in the final scheme given in Fig. 5. In the higher excitation energy region the level density for ^{38}K is rather high (especially above 5 MeV) and, because of the experimental energy resolution of 75 keV, some of the observed triton groups may correspond to multiplets.

Our first aim in the comparison of theory to experiment was to attribute transferred L-values. In fact, in most cases, there is a dominant L-value which implies 3 possible spins. Several calculated curves are given in Fig. 4. They correspond to allowed L-mixtures which best fit the data. In some cases, they may indicate that a particular spin value is more probable; all other L-values can be ruled out.

A summary of our analysis is given in Fig. 5. For comparison we also give the results of Fenton et al.[12] and the compilation by Endt and Van der Leun.[11] One can see that most of the (^{3}He,t) transitions are L=2. The comparison with the one-particle pick-up (^{3}He,α) experiment of Fenton et al. is most significant. More levels have been obtained through the (^{3}He,t) reaction but when there is a correspondence with states obtained through the higher resolution ($\sim$ 40 keV) (^{3}He,α) reaction, the compatibility between the suggested spins and parities is good. The only disagreement concerns the 2.877 MeV state. Keeping the restrictions discussed above in mind, the overlap between the proposed spins and parities in both works can be of interest to get a more precise picture of the level spectrum of ^{38}K.

4. Microscopic Model

We shall consider first one-step transitions only, in order to compare transitions in the sd-shell observed here with transitions in the $f_{7/2}$ shell, which are quite well known.[7] The angular distributions obtained this way obey the parity selection rule $(-)^{\Delta L} = \pi$, and only even L-transfers are allowed. Our macroscopic analysis has already shown this rule is not valid for some transitions. Second-order effects, namely the contributions via the $[(^3He,\alpha) + (\alpha,t)]$ channel will then be included, in order to see whether a better description can be obtained in this way. In this section, we shall again restrict ourselves to the five lowest levels whose structure is fairly well known.[21,22,23]

4.1 FIRST-ORDER TRANSITIONS.

The DWBA amplitude we use for the $(^3He,t)$ reaction has been described in detail in Ref. 7. The transition occurs via an effective projectile-target nucleon interaction

$$V(r) = V_\tau f(r) + V_{\sigma\tau}\, f(r)\, \vec{\sigma}_1 \cdot \vec{\sigma}_2 + V_{T\tau}\, g(r)\, S_{12} \qquad (1)$$

using the notation of Ref. 7.

Our main purpose in this section will be to determine whether the interaction strengths V_τ, $V_{\sigma\tau}$, $V_{T\tau}$ needed to reproduce the magnitudes of the $^{38}Ar(^3He,t)^{38}K$ reaction cross sections are consistent with those obtained for a large selection of other nuclei. It was found previously that the effective interaction needed to describe the $(^3He,t)$ reaction as a one-step process was fairly independent of the particular shell-model level the particles were in.[7] On the other hand, there was a strong

L-dependence (L ≡ angular momentum transfer) which can be explained[2,3,20] by the existence of second-order contributions via the [(^{3}He,α) + (α,t)] process. However, all the transitions considered were of the type: $j=\ell+1/2 \rightarrow j'=\ell'+1/2$ (type 1). The results of Ref. 7 suggested that the properties of the one-step $j=\ell-1/2 \rightarrow j'=\ell'-1/2$ transitions (type 2) were drastically different. The tensor force is very strong for unnatural-parity transitions and dominates for type 1 transitions.[6,7] On the other hand, the tensor force is very weak for type 2 transitions. In other words, using the same values for $V_{\sigma\tau}$ and $V_{T\tau}$ for both type 1 and type 2 transitions results in vastly different cross section magnitudes in an $(f_{7/2} \rightarrow f_{7/2})^{3+}$ and a $(d_{3/2} \rightarrow d_{3/2})^{3+}$ transition, if one considers a single-step mechanism only. A severe test for the adequacy of the one-step description is therefore to check whether both $(d_{3/2} \rightarrow d_{3/2})$ transitions, and $(f_{7/2} \rightarrow f_{7/2})$ transitions, as seen for instance in the ^{42}Ca(^{3}He,t)^{42}Sc and ^{48}Ca(^{3}He,t)^{48}Sc reactions,[5,7,24] can be reproduced by an interaction such as that in Eq. (1) using the same parameters (essentially V_τ for natural parity transitions and $V_{T\tau}$ for unnatural parity transitions). Unfortunately, the only type 2 transitions studied experimentally,[25] $p_{1/2} \rightarrow p_{1/2}$ in ^{14}C(^{3}He,t)^{14}N and ^{14}N(^{3}He,t)^{14}O, indicated that neither a pure central[25] nor a central + tensor[26] force could reproduce the shape of the observed angular distributions. Whether the fault lies with the optical model treatment or with an inadequate description of the transition operator is not clear. However, the measurements do suggest[26] that the central force required for type 2 unnatural-parity transitions is about four times stronger than the upper limit determined[7] from type 1 transitions. It was therefore particularly

interesting to study the $^{38}Ar(^{3}He,t)^{38}K$ reaction to try and clarify the situation.

For type 1 transitions, the previously obtained strengths were[7]:

$$\begin{cases} V_{\tau} \sim 6 \text{ to } 7 \text{ MeV for } L = 0. \\ V_{T\tau} \sim 3 \text{ MeV}. \end{cases}$$

The parameter $V_{\sigma\tau}$ is not well determined, but there is definitely an upper limit[4,7] to its strength since a dominant $\vec{\sigma}_1 \cdot \vec{\sigma}_2$ term would lead to an incorrect angular distribution:[4,6,7]

$$V_{\sigma\tau} \sim 0 \text{ to } 5 \text{ MeV}.$$

In Ref. 7, $V_{\sigma\tau}$ has been arbitrarily taken equal to $V_{T\tau}$. In the analysis we report here the results have also been found to be insensitive to the precise choice of $V_{\sigma\tau}$, and we shall not comment further on the determination of that parameter.

Various descriptions have been proposed for the $0^+ \rightarrow 3^+$ multiplet. According to the wave functions of Dieperink and Glaudemans,[21] or those of Wildenthal et al.[22] which reproduce the observed β transition rates rather well, three of the five ^{38}K levels below 2.4 MeV [3^+ (g.s.), 0^+(0.13 MeV), and 2^+(2.41 MeV)] are mainly built from the $(d_{3/2}^{-2})$ configuration, while the other two levels [1_1^+(0.46 MeV) and 1_2^+(1.70 MeV)] are composed of $(d_{3/2}^{-2})$, $(d_{3/2}^{-1}\ s_{1/2}^{-1})$, and other components. Although Dieperink and Glaudemans,[21] and Wildenthal et al.[22] restrict themselves to configurations composed of two holes in the sd-shell, Skouras[23] allows for two particle-four hole admixtures but considers the T=1 (0^+ and 2^+) states only.

Because the natural-parity transitions depend only on the strength of V_τ, and the unnatural-parity transitions on the strength of $V_{T\tau}$, the values of these parameters are very simply obtained by adjusting the magnitudes of the calculated cross sections to the experimental ones. The results are given in Table II, where a comparison is made with the values obtained for the $f_{7/2}$ transitions in mass 48. The 0.458 MeV (1_1^+) state has not been included, since a one-step process forces the calculated angular distribution to be either an L=0 or L=2 shape, excluding L=1.

Several general features can be noticed. First, the strength required for the 0^+ and 2^+ states is consistent with the one observed [Table II] for the $^{48}Ca(^3He,t)^{48}Sc$ reaction.[24] The calculations of ref. 7 have been redone, using more recent data[24] than those available at the time;[5] they are fairly insensitive to configuration mixing. In the case of the 1^+ and 3^+ states, if one assumes a pure $(d_{3/2}^{-2})$ wave function, the strength needed for the tensor force is much larger (a factor of 3) than the one required for the $f_{7/2}$ transition. This is a huge discrepancy, as the cross sections would be 10 times too small for the ^{38}K states if one used the same strengths as in the case of ^{48}Sc. Configuration mixing, as provided by the wave functions of Dieperink and Glaudemans,[21] leads to a real improvement for the 1^+ state, but does not help to rectify the discrepancy for the 3^+ state. One might wonder whether the absence of (2p-4h) admixtures in the wave functions might be responsible for the remaining gap. Indeed, a transition from the $[(f_{7/2}^2)^{0^+}$-4 hole] configuration in the ^{38}Ar ground state to the $[(f_{7/2}^2)^{3^+}$-4 hole] configuration in the ^{38}K 3^+ state would be rather strong, despite its small weight in the wave function, since the matrix

element of the tensor force S_{12} is much stronger for the $f_{7/2}$ than for the $d_{3/2}$ transition.[7] A rough estimate of these (2p-4h) admixtures for the T=1 status can be obtained from the wave functions of Skouras.[23] In that case, the (2p-4h) component represented about 16% of the wave function. Assuming the proportion of (2p-4h) is the same in the case of the 1^+ and 3^+ states, and choosing the sign of the amplitude to correspond to the most favorable case, one can bring the strength of $V_{T\tau}$ needed for the ^{38}K 3^+ state down to a slightly smaller value [Table II] which is still, however, too large by nearly a factor of 3. (The corresponding angular distribution is shown in Fig. 6.) In addition, the actual magnitude of the (2p-4h) admixtures which contribute to the (^{3}He,t) transition is much smaller[27] than the one we have assumed here; in fact, it is probably negligible.

The $0^+ \rightarrow 1^+$ transition which displays an L=1 pattern cannot be reproduced by any microscopic calculation. This reminds one of the $0^+ \rightarrow 0^+$ transitions which have an L=1 shape.[3,19,20] The similarity between the two cases is remarkable. The L=1 shape of the $0^+ \rightarrow 0^+$ transitions was interpreted[3] as a manifestation of the nearly complete cancellation of the one-step process (due to configuration mixing) which allowed second-order contributions to show up. Indeed, in the case we are concerned with, configuration mixing leads to a destructive interference between the various components of the 0.458 MeV (1^+_1) level, whereas the 1.7 MeV (1^+_2) level displays a constructive interference.

The calculations were carried out using both codes DWBA74[28] and CHUCK.[13] The parameter values were the same, with the exception of $\mu_{T\tau}$. Indeed, to take into account the difference between the

definition of the tensor force in the two codes, one must use two different values for the tensor force range. The results and conclusions were essentially the same in both cases. See Fig. 6 for the microscopic one-step angular distribution calculations.

In summary, the natural-parity transitions are very similar to those already observed, whereas the unnatural-parity, anti-analog states raise two problems: the strength of the 3^+ level and the anomalous shape of the 0.458 MeV (1_1^+) level. Both discrepancies seem to fall beyond the scope of the DWBA, and an investigation of possible second-order contributions is necessary.

4.2 SECOND-ORDER EFFECTS

The transitions occurring via the [(^{3}He,α) + (α,t)] channel can be included in a way which is now rather well known.[20,29,30] We have not solved the whole set of coupled equations, but we have taken into account only the contributions up to second order [Fig. 7]. The intermediate states were assumed to be obtained by simply picking up a particle from the ^{38}Ar ground state without disturbing the others. The spectroscopic amplitude for the (^{3}He,α) process: $S = \langle {}^{37}\mathrm{Ar} | a_n | {}^{38}\mathrm{Ar} \rangle$ is then unity, since $|{}^{37}\mathrm{Ar}\rangle = a_n |{}^{38}\mathrm{Ar}\rangle$ except for small corrections. Also, the spectroscopic amplitude for the (α,t) process: $S_p = \langle {}^{38}\mathrm{K} | a_p^+ | {}^{37}\mathrm{Ar} \rangle = \langle {}^{38}\mathrm{K} | a_p^+ a_n | {}^{38}\mathrm{Ar} \rangle$ is then proportional to the same configuration mixing amplitudes as those which enter into the direct, one-step transition.

All the calculations of the present part of our study were done using the coupled channels code CHUCK.[13]

a) Choice of parameters

If one considers the magnitude of the second-order transition for each of the levels studied, one realizes that it is rather sensitive (the

variation can be a factor of 2, in some cases) to the choice of optical parameters. Obviously the parameter set which gave us the best overall agreement with the experimental angular distributions of the five lowest levels of ^{38}K in a one-step calculation is not necessarily the best choice if second-order effects are included. To illustrate this point with an example, we can consider the following alternatives: If we want to get reasonable two-step transition magnitudes using set a) of Table I, we have to use the optical parameters suggested by Toyama[20] (or similar ones) for the α particle, with a one-particle transfer strength D_o=480 MeV-fm$^{3/2}$. If we use set d) in Table I, we should choose the V_R=397.3 MeV or V_R=266.4 MeV sets suggested by Weisser et al.[31] for the α particle, with a D_o which is smaller than 400 MeV-fm$^{3/2}$ and even less for smaller values of V_R. (This behavior is very unfortunate. We have had problems in finding optical parameters consistent with the known value of D_o since large cross sections are usually obtained. The explanation for this behavior can probably be found in Ref. 32, which appeared after our work was completed.) As it is commonly accepted that the optical model V_R should be close to 200 MeV for α particles and as the parameter $D_o \approx 480$ MeV-fm$^{3/2}$ is fairly well known, we shall restrict ourselves to the parameters listed in Table III. One should note that our ^3He and triton optical parameter sets are very similar to the ones used by Toyama[2] and indeed they give comparable results; we prefer to keep our own parameters in order to assure consistency with the previous sections of our work. One remembers that the only real advantage, however small, of using set d) of Table I instead of set a) concerned the slope of the calculated curve for the 2^+ level of ^{38}K. It will be shown shortly, however, that the introduction of second-order transitions in our calculations removes this difficulty. Therefore, we feel justified in our choice of parameters for the second-order transitions [see Table III].

b) $^{38}Ar(^{3}He,t)\,^{38}K$

Whatever optical parameters are chosen, the second-order transition dominates the 3^+ state when the tensor strength is adjusted to fit the $^{48}Ca \rightarrow {}^{48}Sc\ 3^+$ transition. Using the parameters of Table III, the second-order contribution has about the right magnitude for the 3^+ state of ^{38}K. This gives us a prediction for the two-step process which shall no longer be modified. Figure 8 shows the theoretical results for the direct, two-step and combined processes, as well as experimental measurements for each of the five lowest levels of ^{38}K. One can see that, in the case of the 0^+ and 2^+ levels, the second-order contribution alone is a factor of 2 too small at forward angles, but has the correct magnitude at angles beyond 30°, where the calculations involving a direct mechanism fit poorly. Also, if a central force $V_\tau = 12.5$ MeV is used for both levels, one-step contributions provide just the missing strength at forward angles, and the interference between the two amplitudes leads to angular distributions in which both forward- and backward-angle experimental patterns are qualitatively reproduced. Thus, in the case of natural-parity states, it is possible to describe both levels using exactly the same parameters. In particular, one should notice that the lack of structure and the slope of the 2^+ level are well reproduced. [The theoretical results which are shown in the case of the 2^+ level have been obtained by using the wave functions of Dieperink and Glaudemans[21]; this leads to a better agreement than that obtained by simply assuming a $(d_{3/2}^{-2})$ configuration.] As far as the unnatural-parity states are concerned, the two-step contribution alone explains the observed strength of both the 0.458 MeV 1_1^+ and 3^+ ground state, which could not be reproduced by a one-step calculation; on the other hand the second-order effect is too small by an order of magnitude for the

1.704 MeV (1_2^+) state. Once again, we shall not discuss the value of the parameter $V_{\sigma\tau}$; that term of the force contributes only weakly to our transitions. If one uses a tensor force $V_{T\tau}$ = 7 MeV for the 3^+ and both 1^+ levels, all these unnatural-parity states can be reproduced quite well. In this case also, it is possible to describe all the levels by using the same parameters. It should nevertheless be acknowledged that while the magnitude of the 0.458 MeV (1_1^+) level is quite satisfactory and the shape is qualitatively reproduced, the precise form remains a problem. In brief, it seems we are fully justified to conclude that two-step processes including an intermediate α particle are essential to explain the experimental results concerning the $^{38}Ar(^3He,t)^{38}K$ reaction at 40 MeV. However a more elaborate treatment of the second-order process still seems necessary.[32,33]

c) $^{48}Ca(^3He,t)^{48}Sc$.

As the specific choice of the different parameters has been shown to be crucial, we felt it was important to test the various values we used for A = 38 in the case of A = 48. Figure 9 shows the theoretical curves for direct, two-step and combined transitions, together with experimental data. We show results for all $(f_{7/2} \rightarrow f_{7/2})_{0^+ \rightarrow 7^+}$ transitions in the $^{48}Ca(^3He,t)^{48}Sc$ reaction. Toyama[2] discussed this reaction previously, but restricted himself to natural-parity levels and to separate two-step and direct transitions. In our case, the strengths we have used to describe the (^{3}He,t) mechanism for A = 38 are consistent with the requirements for A = 48. The theoretical cross sections are in satisfactory agreement with the experimental ones and the shapes of the theoretical curves are quite good. Our results are correct within a

factor of 2: the natural-parity transitions are somewhat too weak, whereas the unnatural-parity transitions are slightly too strong. If we made the choice $V_\tau \sim 15$ MeV and $V_{T\tau} \sim 5$ MeV, we would reproduce the exact strength of the transitions to these 8 levels. We consider that a justification of the choice we made for the different parameters has been provided and that the apparent discrepancy between the two types of (^{3}He,t) transitions[7] has been greatly reduced. In table 4 the final values of V_τ and $V_{T\tau}$ are given. They are now nearly unique for all spins and targets.

5. Conclusion

In the first part of our study, we have been able, using a macroscopic model, to help clarify the interpretation of the dense level spectrum of ^{38}K. In the second part of the present paper convincing evidence has been given for the importance of a "combined" process in the explanation of (^{3}He,t) transitions. Indeed, it is necessary to include both a direct charge-exchange reaction and the transitions via an intermediate α particle in the calculations in order to obtain a satisfactory description of the mechanism of the (^{3}He,t) reaction.

ACKNOWLEDGMENTS

One of us (CJZ) wishes to express his hearty thanks to the French Government for financial support and to the I.S.N. (Grenoble) and the C.E.N. (Saclay) for the competent attention, sympathy and computing facilities, provided to him throughout his "Doctorat de troisieme cycle" work.

FOOTNOTES AND REFERENCES

* This work was done with support from Division of Nuclear Science, Nuclear Physics Division, U.S. Department of Energy.

+ Present address: CEN Saclay, B.P. No. 2, Gif-sur-Yvette, FRANCE

++ Present address: Physics Department, Indiana University, Bloomington, IN. 47401.

+++ Boursier du Governement Francais — Present address: Department of Physics and Astronomy, University College, London, England.

1. In particular, see Argonne National Laboratory Informal Report No. PHY-1970A, January 1970, and references contained therein.
2. M. Toyama, Phys. Lett. 38B, 147 (1972).
3. G. Bertsch and R. Schaeffer, Phys. Lett. 38B, 159 (1972).
4. P. Kossanyi-Demay, P. Roussel, H. Faraggi, and R. Schaeffer, Nucl. Phys. A148, 181 (1970).
5. G. Bruge, A. Bussiere, H. Faraggi, P. Kossanyi-Demay, J. M. Loiseaux, P. Roussel, and L. Valentin, Nucl. Phys. A129, 417 (1969).
6. E. Rost and P. D. Kunz, Phys. Lett. 30B, 231 (1969).
7. R. Schaeffer, Nucl. Phys. A164, 145 (1971).
8. R. Sherr, T. S. Bhatia, D. Cline, and J. J. Schwartz, Ann. of Phys. 66, 548 (1971).
9. J. R. Comfort, J. P. Schiffer, A. Richter, and M. M. Stautberg, Phys. Rev. Lett. 26, 1338 (1971).
10. J. M. Loiseaux, G. Bruge, P. Kossanyi-Demay, Ha Duc Long, A. Chaumeaux, Y. Terrien, and R. Schaeffer, Phys. Rev. C 4, 1219 (1971).
11. P. M. Endt and C. Van der Leun, Nucl. Phys. A214, 403 (1973).

12. J. A. Fenton, T. H. Kruse, N. Williams, M. E. Williams, R. N. Boyd, and W. Savin, Nucl. Phys. A187, 123 (1972).

13. P. D. Kunz and E. Rost, Program CHUCK, University of Colorado, Boulder, Colo. (unpublished).

14. F. S. Goulding, D. A. Landis, J. Cerny, and R. H. Pehl, Nucl. Instr. Methods 31, 1 (1964).

15. P. D. Kunz, Program DWUCK, University of Colorado, Boulder, Colo. (unpublished).

16. J. W. Leutzelschwab, and J. C. Hafele, Phys. Rev. 180, 1023 (1969).

17. E. F. Gibson, B. W. Ridley, J. J. Kraushaar, M. E. Rickey, and R. H. Bassel, Phys. Rev. 155, 1194 (1967).

18. J. C. Hafele, E. R. Flynn, and A. G. Blair, Phys. Rev 155 1238 (1967).

19. R. A. Hinrichs, R. Sherr, G. M. Crawley, and I. Proctor, Phys. Rev. Lett. 25, 829 (1970).

20. W. R. Coker, T. Udagawa, and H. H. Wolter, Phys. Lett. 41B, 237 (1972); Phys. Rev. C 7, 1154 (1973); and Phys. Lett. 46B, 27 (1973).
N. B. De Takacsy, Phys. Lett. 42B, 1 (1972).
M. Toyama, Nucl. Phys. A211, 254 (1973).

21. A.E.L. Dieperink, and P.W.M. Glaudemans, Phys. Lett. 28B, 531 (1969).

22. B. H. Wildenthal, E. C. Halbert, J. B. McGrory, and T.T.S. Kuo, Phys. Rev. C 4, 1267 (1971) [wave functions closely similar to those in Ref. 21].

23. L. D. Skouras, Phys. Lett. 31B, 439 (1970), and private communication.

24. A. Richter, J. R. Comfort, V. Anantaraman, and J. P. Schiffer, Phys. Rev. C 5, 821 (1972).

25. G. C. Ball and J. Cerny, Phys. Rev. 177, 1466 (1969).

26. R. Schaeffer, unpublished calculations based on the data in Ref. 25.

27. L. D. Skouras, private communcation.

28. R. Schaeffer, J. Raynal, program DWBA74, CEN Saclay (unpublished).

29. L. D. Rickertsen, M. J. Schneider, J. J. Kraushaar, W. R. Zimmermans, and H. Rudolph, to be published.

30. L. D. Rickertsen and P. D. Kunz, Phys. Lett. 47B, 11 (1973).

31. D. C. Weisser, J. S. Lilley, R. K. Hobbie, and G. W. Greenlees, Phys. Rev. C 2, 544 (1970).

32. L. A. Charlton and P. D. Kunz, Phys. Lett. 72B, 7 (1977).

33. F. Osterfeld, T. Udagawa, and H. H. Wolter, Nucl. Phys. A278, 1 (1977).

Table I

^{3}He and Triton Optical Potentials Used in the Present Calculations

Particle	Set	V (MeV)	r_v (fm)	a_v (fm)	W (MeV)	r_w (fm)	a_w (fm)	W_s (MeV)	r_{ws} (fm)	a_{ws} (fm)
^{3}He [a]	a	150.7	1.22	0.7	23.5	1.5	0.8	-0.96	1.5	0.8
t [a]	a	143.7	1.20	0.7	23.5	1.5	0.8	0.96	1.5	0.8
^{3}He [b]	d	175.2	1.145	0.784	13.96	1.587	0.633			
t [c]	d	152	1.24	0.684	19.6	1.48	0.771			

a) Ref. 5

b) Ref. 17

c) Ref. 18

Table II.

Interaction strengths needed for the various calculations described in the caption to Fig. 6. The numbers in parentheses correspond to an approximate estimate of the 2p-4h admixtures in the wave functions, (label S + A in Fig. 6).

Level	$(d_{3/2} \rightarrow d_{3/2})$	Dieperink and Glaudemans	Skouras $(f_{7/2} \rightarrow f_{7/2})$ [a]		
0^+	6	6	6	6.5	V_τ (MeV)
2^+	9.5	7.5	9	9	V_τ (MeV)
1^+	11.5	4.5	(4.5)	3.5	$V_{T\tau}$ (MeV)
3^+	16.5	25	(14)	5	$V_{T\tau}$ (MeV)

μ_τ = 1.415 fm. $\mu_{T\tau}$ = 0.878 fm (DWBA74)

$\mu_{T\tau}$ = 1.415 fm (CHUCK)

a) Taken from the $^{48}Ca(^3He,t)$ reaction (see text).

Table III.

Parameters Used in the Present Calculation which Allow for Two-Step Processes. (See Text)

Set	Particle	V	r_v	a_v	W	r_w	a_w	V_{so}	r_{so}	a_{so}
B+T	$^3He,t$ [a)]	[See Table I, set a)]								
	α [b,c)]	198.6	1.458	0.502	19.8	1.51	0.79			
	α [b,d)]	183.7	1.4	0.56	26	1.48	0.56			
Boulder	^3He [e)]	149.0	1.2	0.72	32.2	1.4	0.88	10	1.2	0.72
	t [e)]	159.2	1.2	0.72	41.5-0.32E	1.4	0.84	10	1.2	0.72
	α [e)]	200	1.4	0.57	55.2-0.6E	1.4	0.57			

a) Ref. 5

b) Ref. 2

c) A = 38

d) A = 48

e) Ref. 31

Table IV

Strength Parameters for the One-Step Effective Interaction Contributing to the (^{3}He,t) Reaction

Configuration	V_T (MeV)	V_{TT} (MeV)
$d_{3/2} \rightarrow d_{3/2}$	12.5	7
$f_{7/2} \rightarrow f_{7/2}$	15	5

Figure Captions

Fig. 1 Triton energy spectrum from the $^{38}Ar(^{3}He,t)^{38}K$ reaction at $\theta_{\ell} = 14°$.

Fig. 2 Choice of the best optical potential parameters using the experimental 0.13 MeV (0^+, T=1) IAS of ^{38}K as a probe of their adequacy. a) Ref. 5, b) Ref.16, c) Refs. 17,18, d) Refs. 17,18 with r_{oc} = 1.25 fm.

Fig. 3 Macroscopic calculations for the g.s. (3^+), 0.458 MeV (1_1^+), 1.704 MeV (1_2^+) and 2.405 MeV (2^+) states of ^{38}K, using two of the optical potential sets selected from Fig. 2. (See Table I.)

Fig. 4 a) and 4b) Experimental and calculated angular distributions for the higher-lying states of ^{38}K using macroscopic calculations only.

Fig. 5 Level scheme of ^{38}K. The results of our work are compared to the data of Fenton et al.[12] and the compilation of Endt and Van der Leun.[11]

Fig. 6 Microscopic calculations for the lowest five levels of ^{38}K. The curves labelled (3/2 3/2) correspond to pure $d_{3/2}^{-2}$ wave functions, those labelled DG to the sd-shell wave functions of Dieperink and Glaudemans[21]; those labelled S + A to the approximate estimate of the 2p-4h admixtures in the Skouras[23] wave functions. The microscopic interaction used is discussed in the text.

Fig. 7 Coupling scheme for the second-order transitions via the pickup channels. The ^{37}Ar states are "model states" in the sense that they are obtained by removing a particle in the true ^{38}Ar ground state without disturbing the other nucleons.

Fig. 8 Microscopic calculations ($V_T = 12.5$ MeV, $V_{T\tau} = 7$ MeV) for the lowest five levels of ^{38}K, allowing for two-step transitions. Curves for the direct, two-step and combined processes are shown. The microscopic interaction used is described in the text. The optical parameters are given in Table III.

Fig. 9 Microscopic calculations ($V_T = 15$ MeV, $V_{T\tau} = 5$ MeV) for the $f_{7/2}$ multiplet $0^+ \rightarrow 7^+$ of ^{48}Sc, allowing for two-step transitions: a) natural parity states; b) unnatural parity states. Curves for the direct, two-step and combined processes are shown, together with experimental data taken from Ref. 24. The microscopic interaction used is described in the text. The optical parameters are given in Table III.

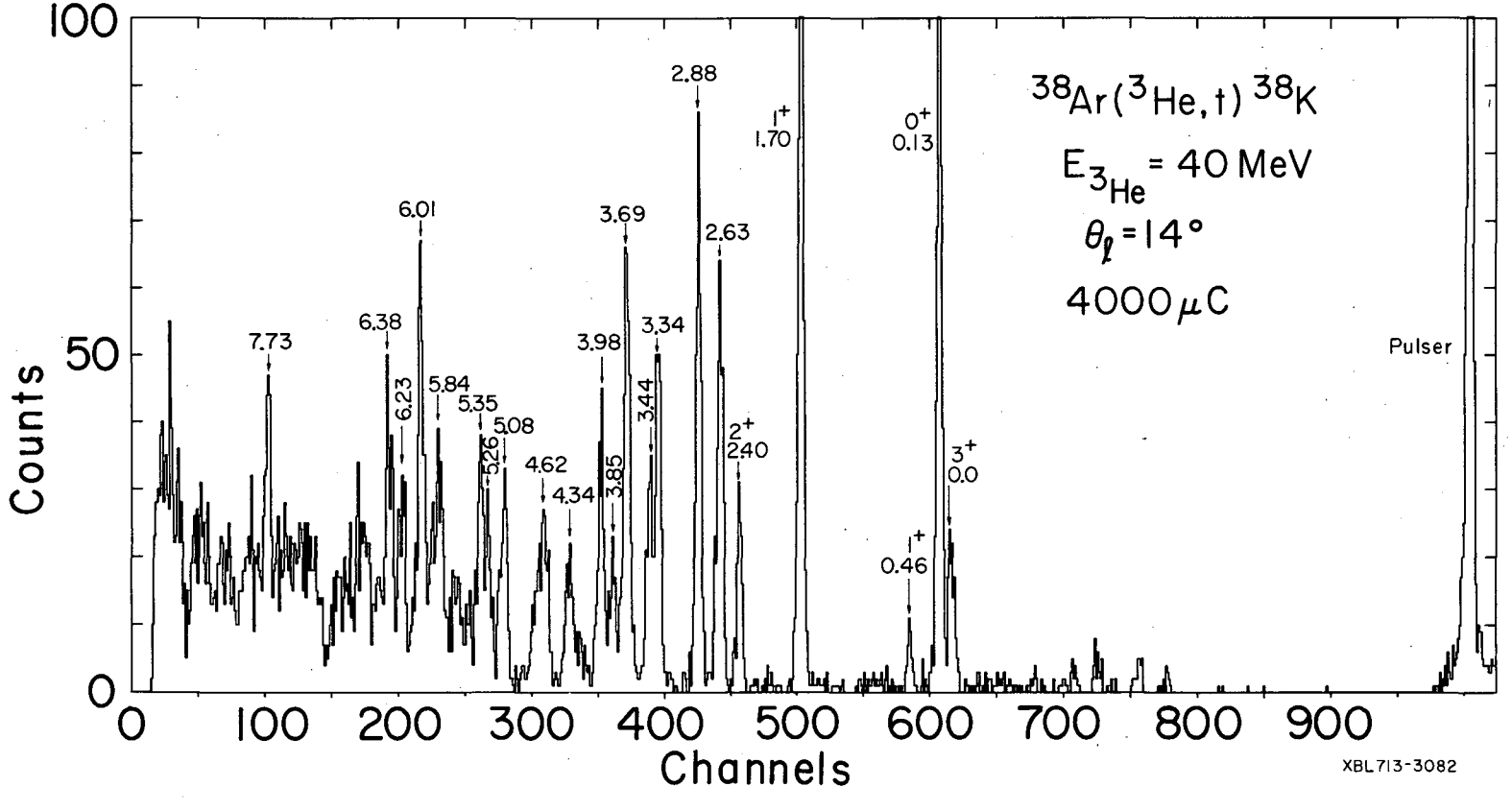

Fig. 1

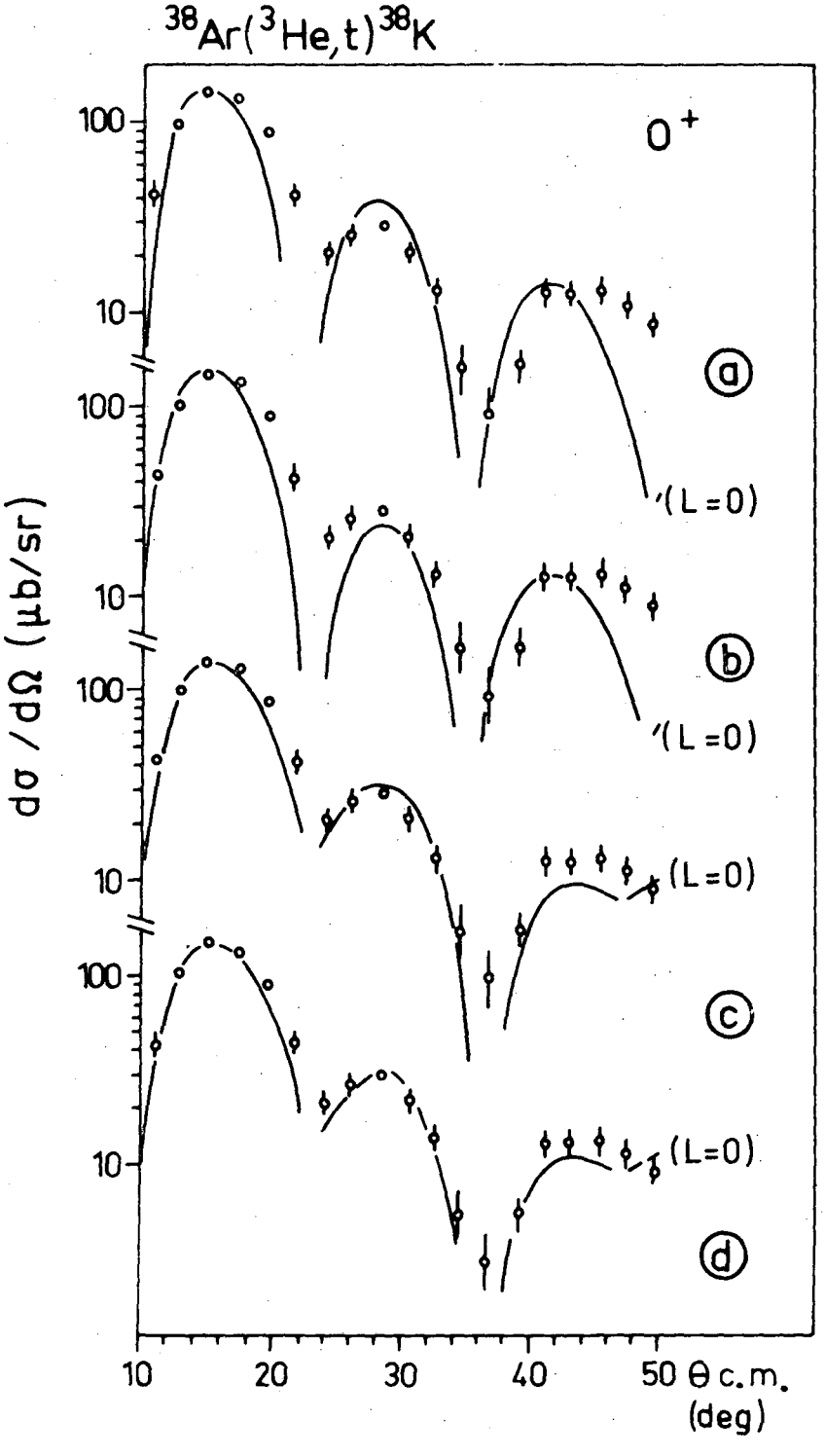

XBL 777-9744

Fig. 2

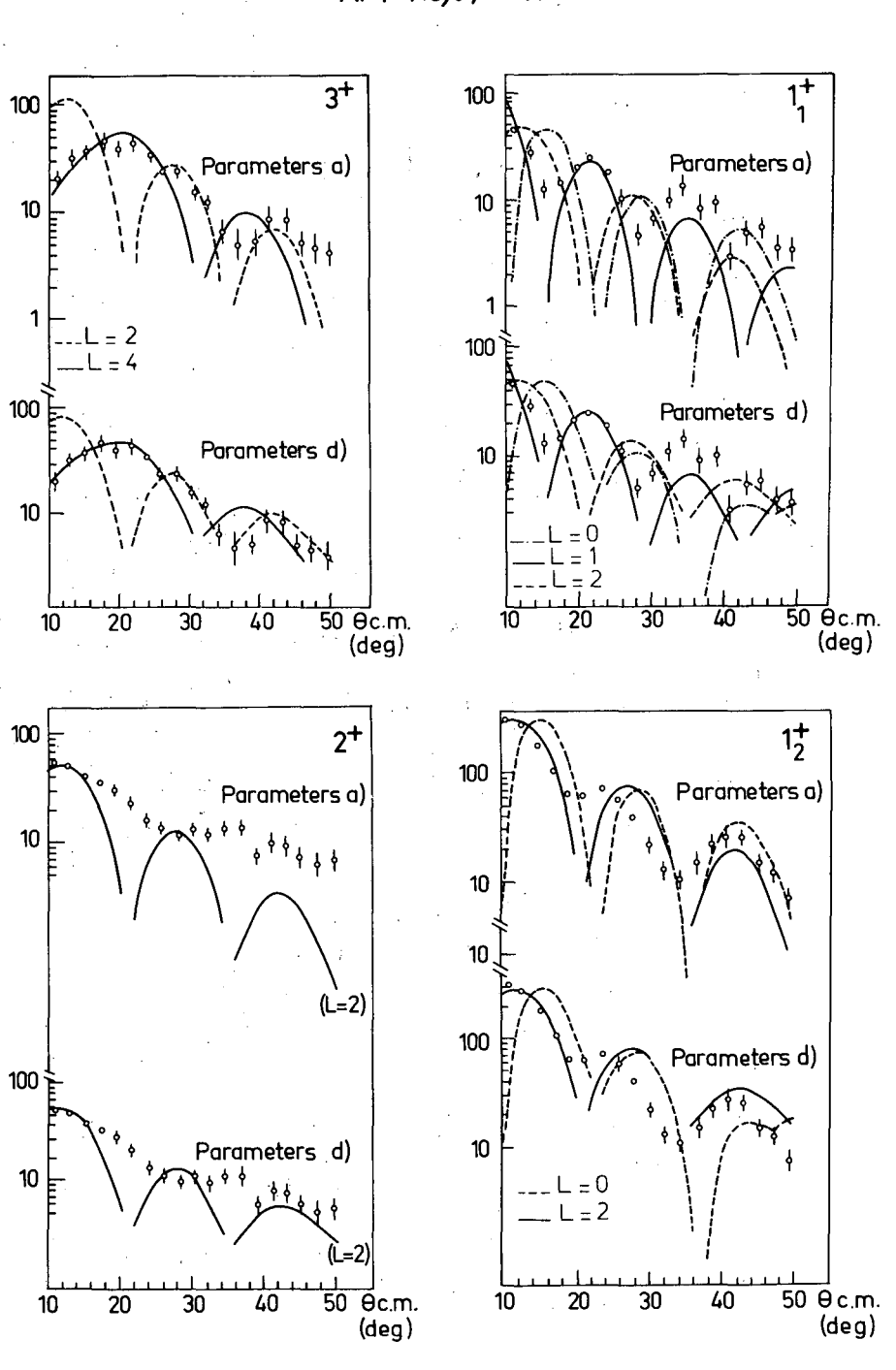

XBL 783-7639

Fig. 3

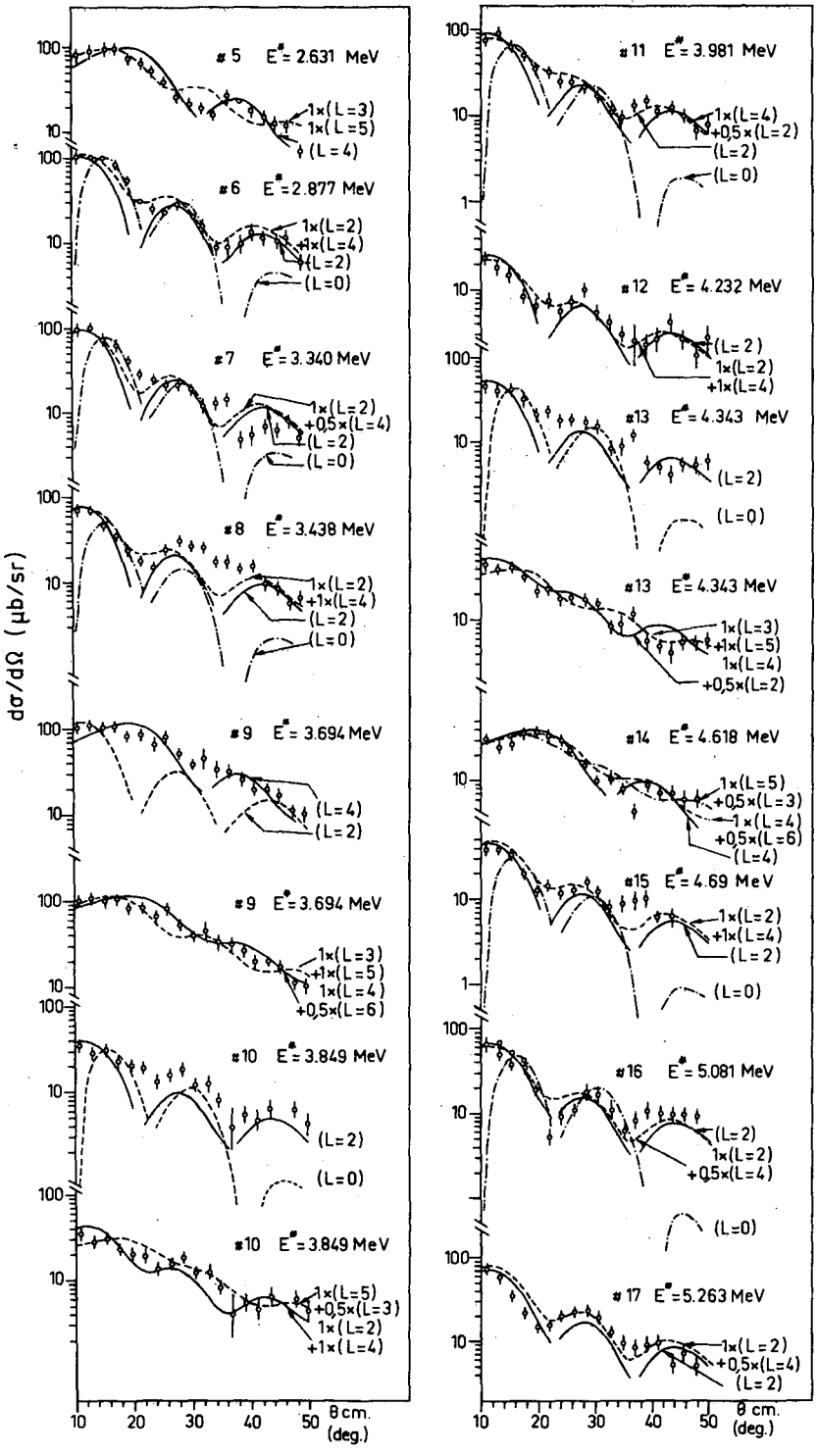
dσ/dΩ (μb/sr)
θ cm. (deg.)
#5 E*= 2.631 MeV
1×(L=3)
1×(L=5)
+(L=4)
#6 E*= 2.877 MeV
1×(L=2)
+1×(L=4)
+(L=2)
(L=0)
#7 E*= 3.340 MeV
1×(L=2)
+0,5×(L=4)
(L=2)
(L=0)
#8 E*= 3.438 MeV
1×(L=2)
+1×(L=4)
(L=2)
(L=0)
#9 E*= 3.694 MeV
(L=4)
(L=2)
#9 E*= 3.694 MeV
1×(L=3)
+1×(L=5)
1×(L=4)
+0,5×(L=6)
#10 E*= 3.849 MeV
(L=2)
(L=0)
#10 E*= 3.849 MeV
1×(L=5)
+0,5×(L=3)
1×(L=2)
+1×(L=4)
#11 E*= 3.981 MeV
1×(L=4)
+0,5×(L=2)
(L=2)
(L=0)
#12 E*= 4.232 MeV
(L=2)
1×(L=2)
+1×(L=4)
#13 E*= 4.343 MeV
(L=2)
(L=0)
#13 E*= 4.343 MeV
1×(L=3)
+1×(L=5)
1×(L=4)
+0,5×(L=2)
#14 E*= 4.618 MeV
1×(L=5)
+0,5×(L=3)
1×(L=4)
+0,5×(L=6)
(L=4)
#15 E*= 4.69 MeV
1×(L=2)
+1×(L=4)
(L=2)
(L=0)
#16 E*= 5.081 MeV
(L=2)
1×(L=2)
+0,5×(L=4)
(L=0)
#17 E*= 5.263 MeV
1×(L=2)
+0,5×(L=4)
(L=2)
XBL 783-7641

Fig. 4a

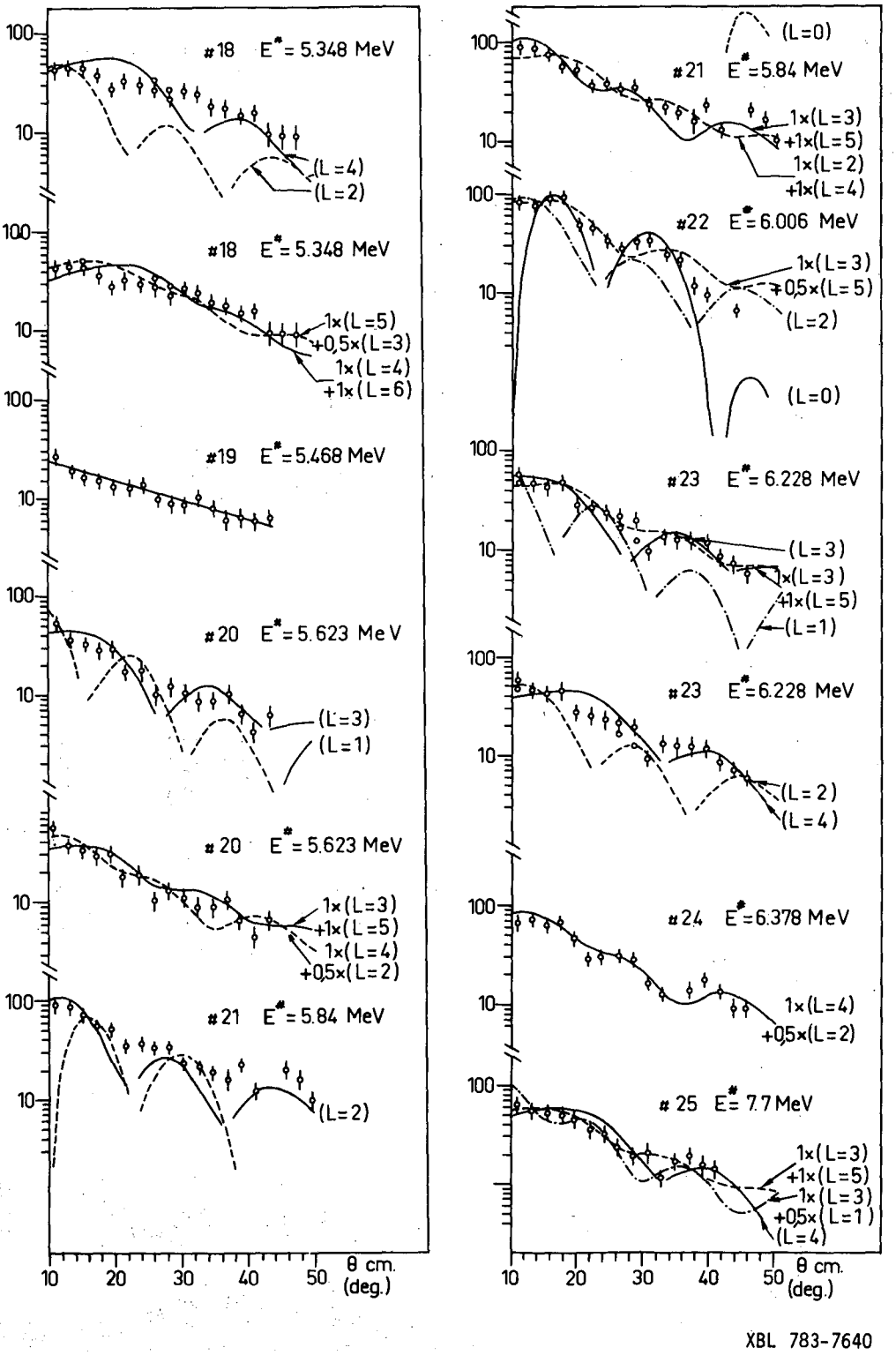

Fig. 4b.

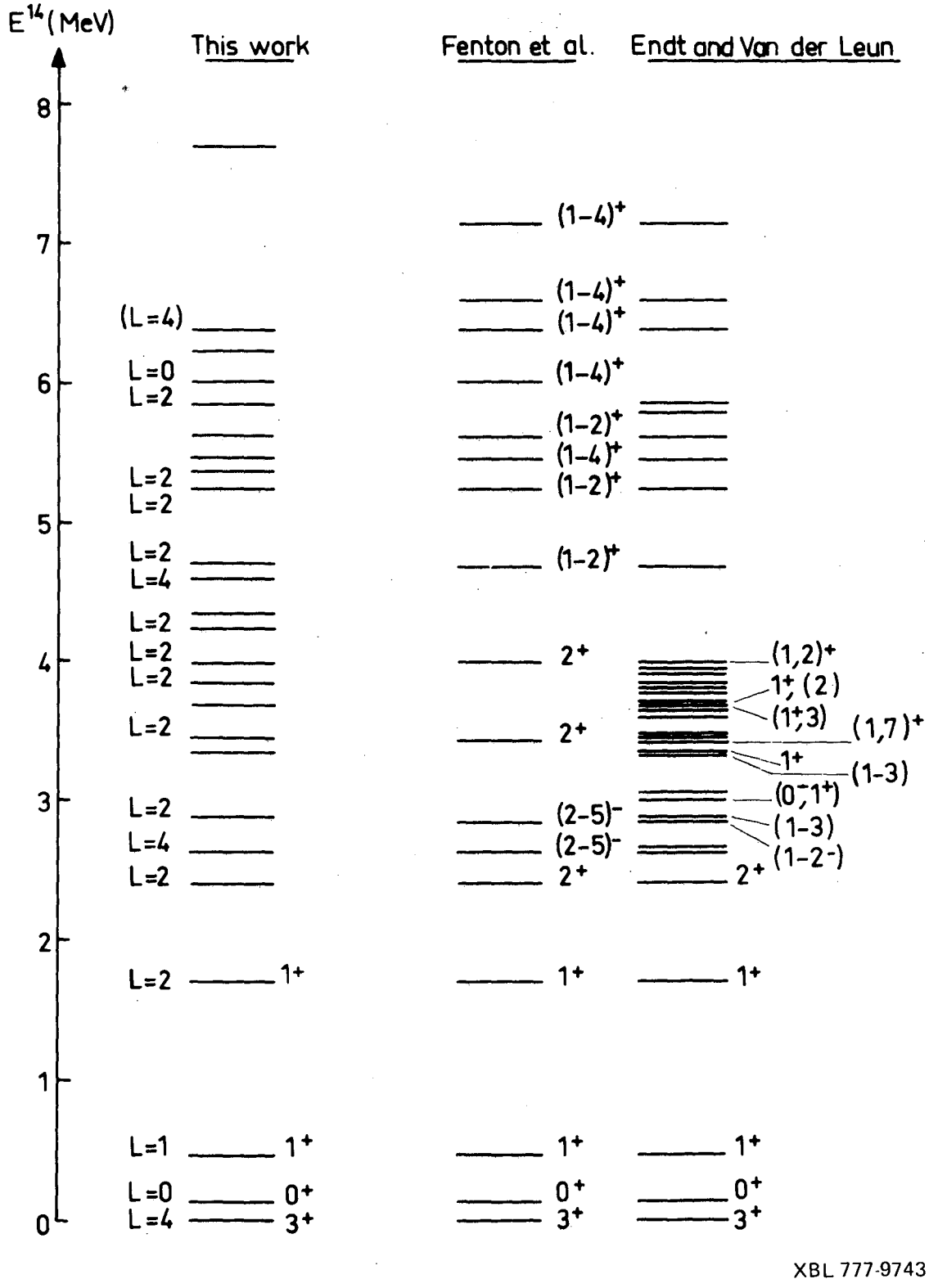
E14 (MeV)
This work
Fenton et al.
Endt and Van der Leun
8
7
6
5
4
3
2
1
0
(L=4)
L=0
L=2
L=2
L=2
L=2
L=2
L=2
L=2
L=2
L=4
L=2
L=2
L=4
L=2
L=1
L=0
L=4
1+
0+
3+
(1-4)+
(1-4)+
(1-4)+
(1-4)+
(1-2)+
(1-4)+
(1-2)+
(1-2)+
2+
2+
(2-5)-
(2-5)-
2+
1+
1+
0+
3+
(1,2)+
1+; (2)
(1+;3)
(1,7)+
1+
(1-3)
(0-;1+)
(1-3)
(1-2-)
2+
1+
1+
0+
3+
XBL 777-9743

Fig. 5

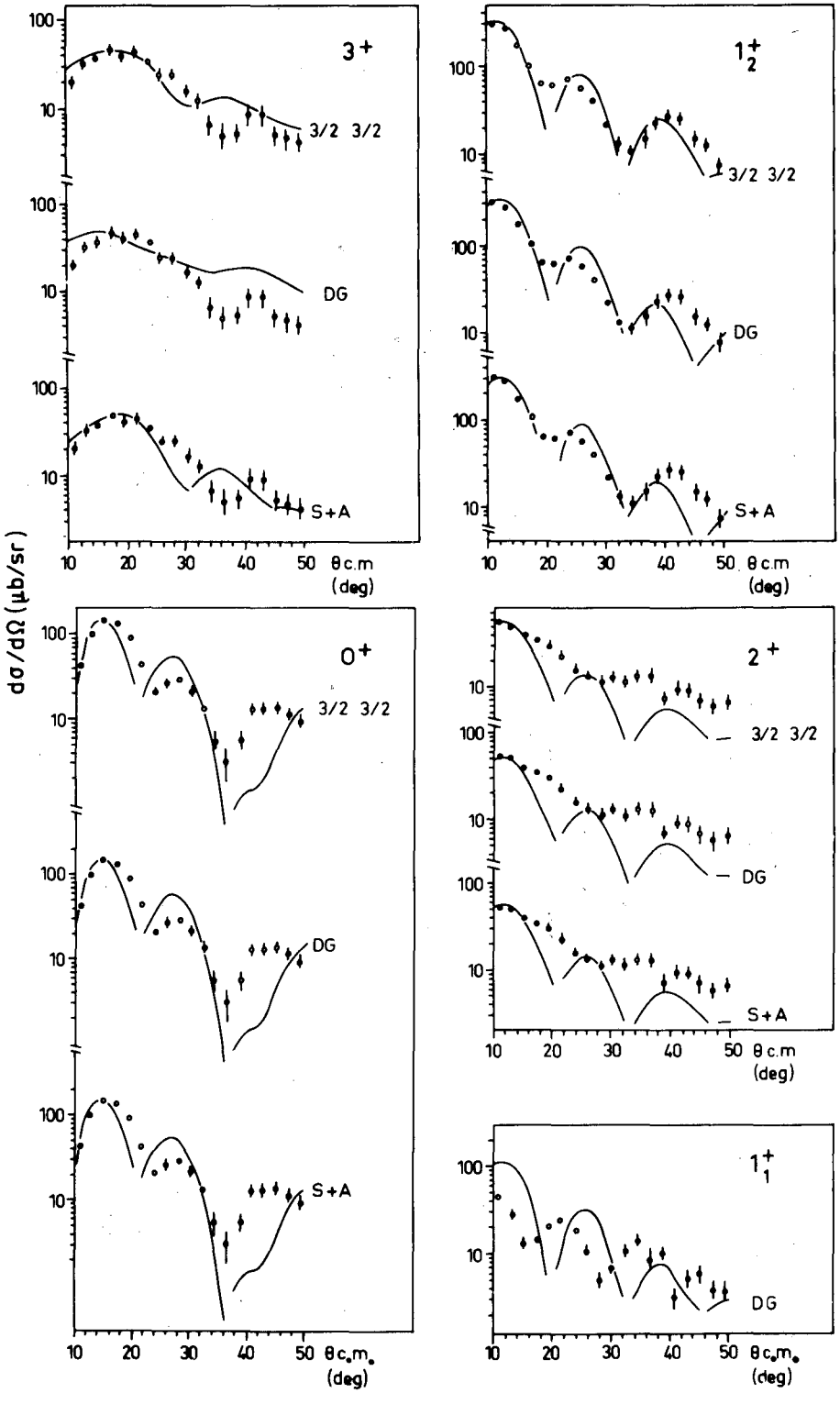

Fig. 6

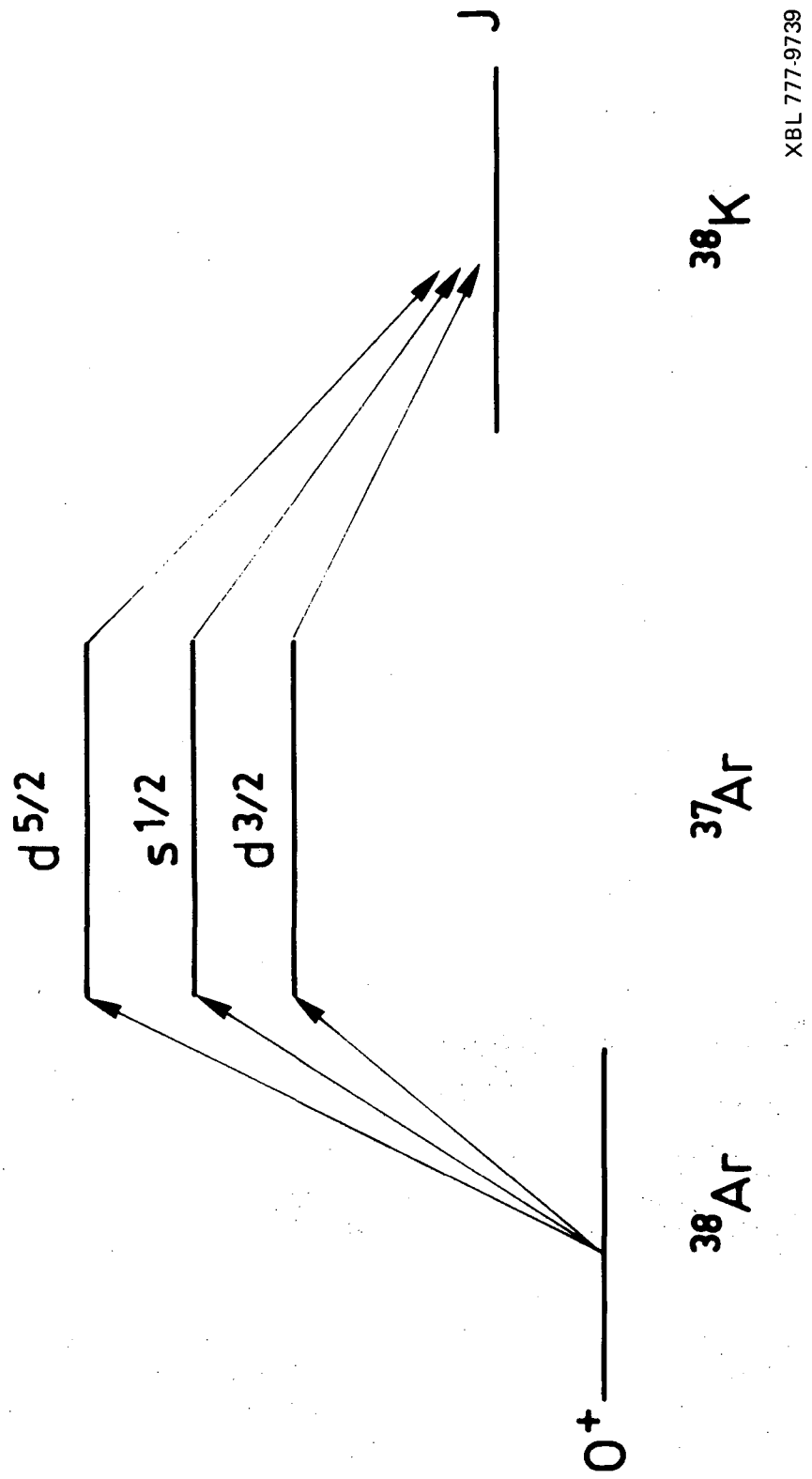

Fig. 7

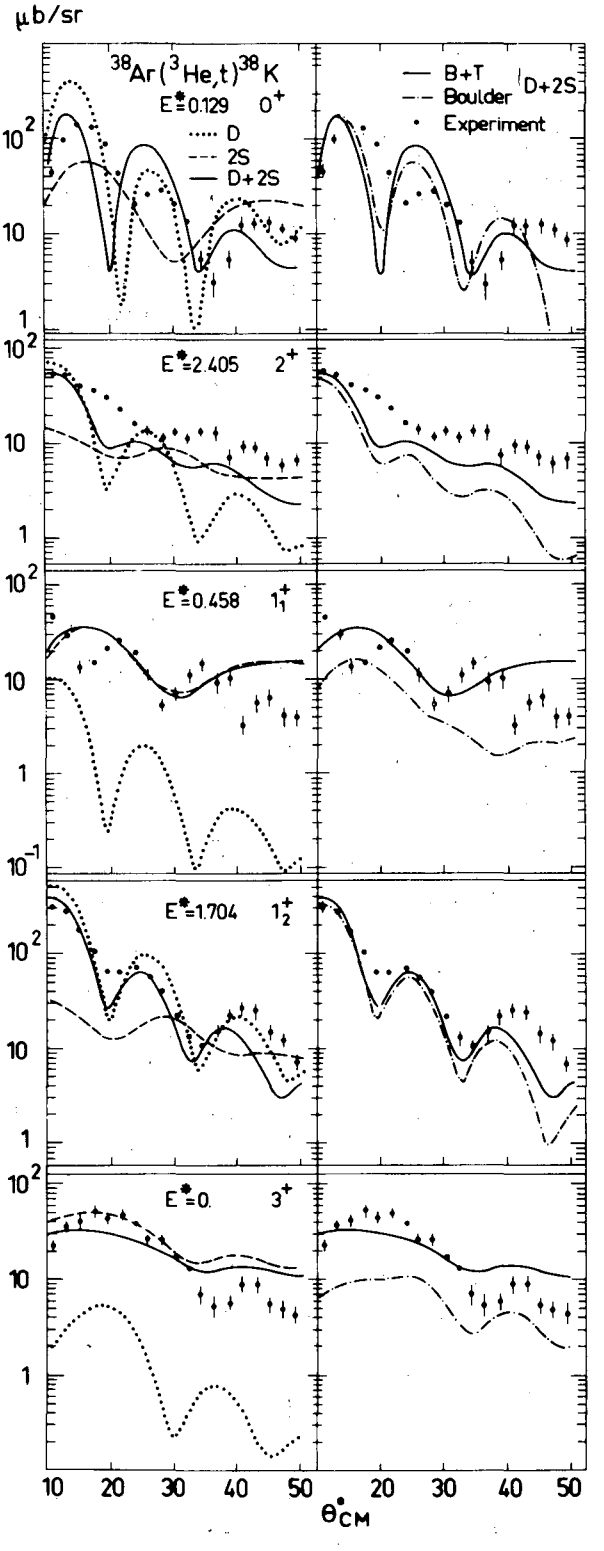

XBL 777-9742

Fig. 8

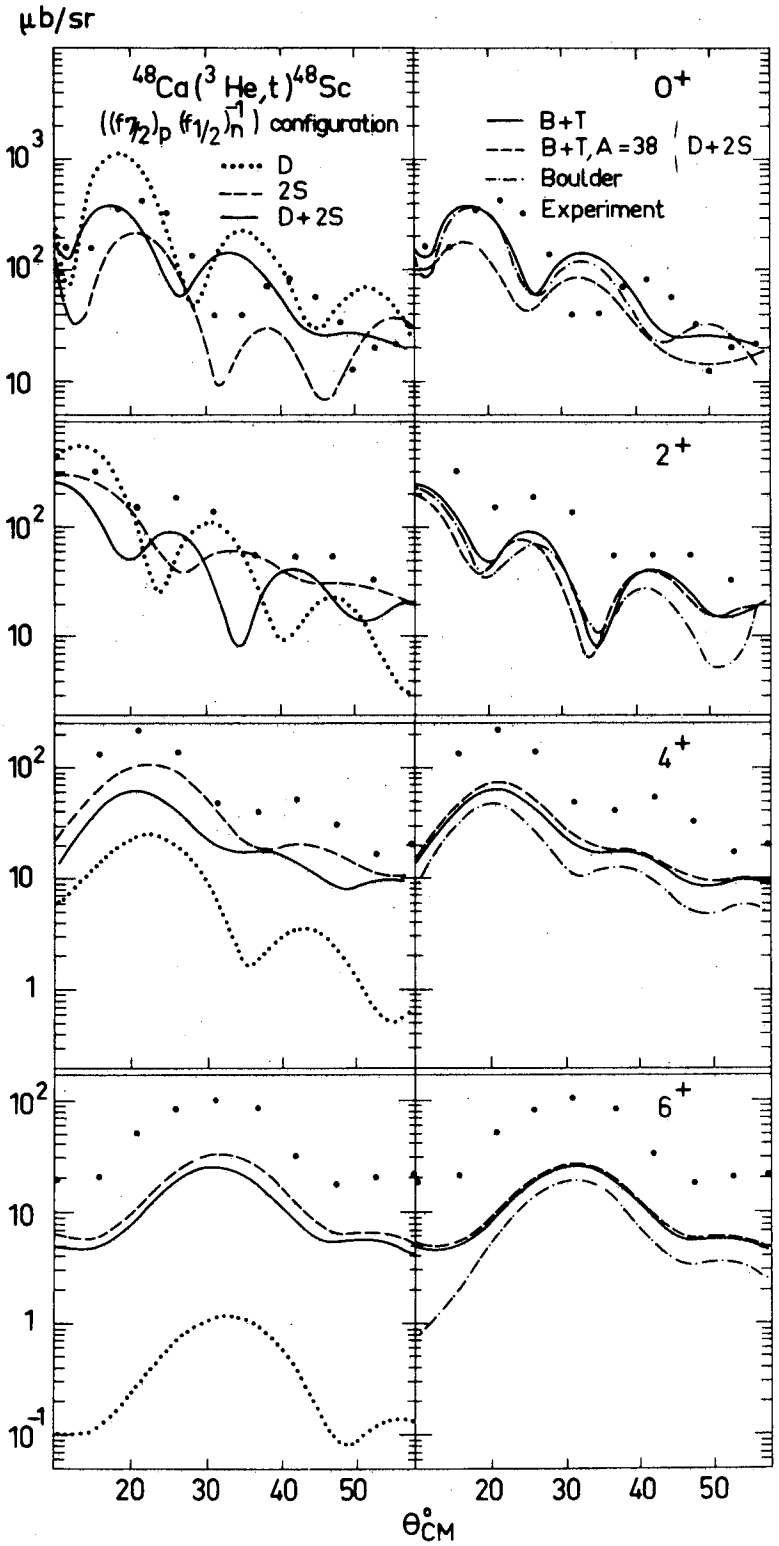

XBL 777-9741

Fig. 9a.

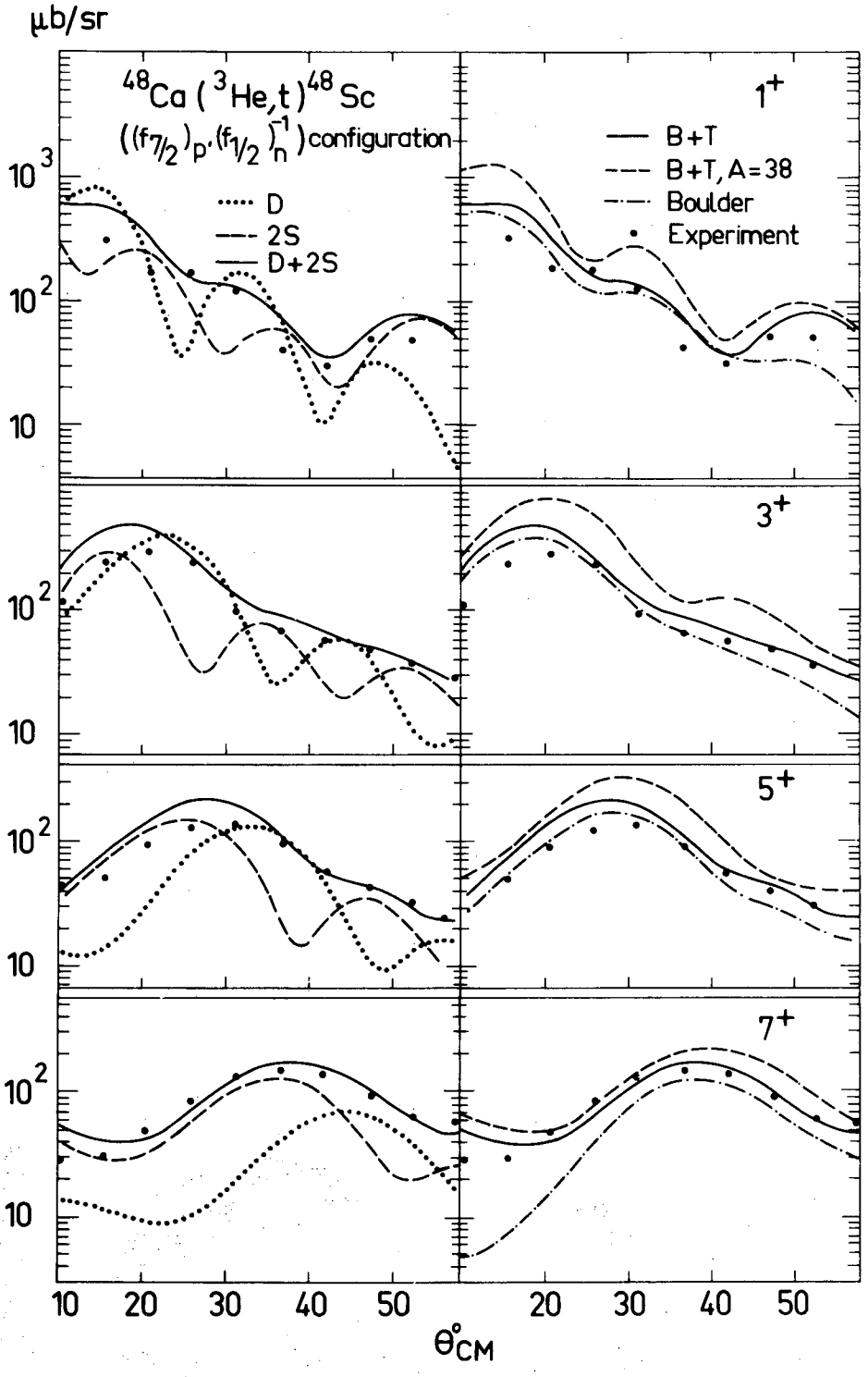

XBL 777-9740

Fig. 9b.

This report was done with support from the Department of Energy. Any conclusions or opinions expressed in this report represent solely those of the author(s) and not necessarily those of The Regents of the University of California, the Lawrence Berkeley Laboratory or the Department of Energy.

TECHNICAL INFORMATION DEPARTMENT
LAWRENCE BERKELEY LABORATORY
UNIVERSITY OF CALIFORNIA
BERKELEY, CALIFORNIA 94720